Modelling of Wave Propagation in Wire Media Using Spatially Dispersive Finite-Difference Time-Domain Method: Numerical Aspects

Yan Zhao, *Student Member, IEEE*, Pavel A. Belov, *Member, IEEE*, and Yang Hao, *Senior Member, IEEE*

***Abstract*—The finite-difference time-domain (FDTD) method is applied for modelling of wire media as artificial dielectrics. Both frequency dispersion and spatial dispersion effects in wire media are taken into account using the auxiliary differential equation method. According to the authors' knowledge, this is the first time when the spatial dispersion effect is considered in the FDTD modelling. The stability of developed spatially dispersive FDTD formulations is analyzed through the use of von Neumann method combined with the Routh-Hurwitz criterion. The results show that the conventional stability Courant limit is preserved using standard discretization scheme for wire media modelling. Flat sub-wavelength lenses formed by wire media are chosen for validation of proposed spatially dispersive FDTD formulation. Results of the simulations demonstrate excellent sub-wavelength imaging capability of the wire medium slabs. The size of the simulation domain is significantly reduced using the modified perfectly matched layer (MPML) which can be placed in close vicinity of the wire medium. It is demonstrated that the reflections from the MPML-wire medium interface are less than -70 dB, that lead to dramatic improvement of convergence compared to conventional simulations.**

***Index Terms*—Artificial dielectrics and metamaterials, finite-difference time-domain (FDTD), spatial dispersion, wire medium.**

I. Introduction

THE wire medium is an artificial material formed by a regular lattice of ideally conducting wires (see Fig. 1). The radii of wires are assumed to be small compared to the lattice periods and the wavelength. The wire medium has been known for a long time [1]–[3] as an artificial dielectric with plasma-like frequency dependent permittivity, but only recently it was shown that this dielectric is non-local and possesses also strong spatial dispersion even at very low frequencies [4]. Following [4] the wire medium can be described (if lattice periods are much smaller than the wavelength) as a uniaxial dielectric with both frequency and spatially dependent effective permittivity

$$\bar{\bar{\varepsilon}} = \varepsilon(k, q_x)\mathbf{xx} + \mathbf{yy} + \mathbf{zz}$$
$$\varepsilon(k, q_x) = \varepsilon_0 \left(1 - \frac{k_0^2}{k^2 - q_x^2}\right) \tag{1}$$

where $k_0 = \omega_0/c$ is the wave number corresponding to the plasma frequency ω_0, $k = \omega/c$ is the wave number of free space, c is the speed of light, and q_x is the component of wave vector $\mathbf{q}$ along the wires. The dependence of permittivity (1) on q_x represents the spatial dispersion effect which was not taken into account in the conventional local uniaxial model of wire medium [1]–[3].

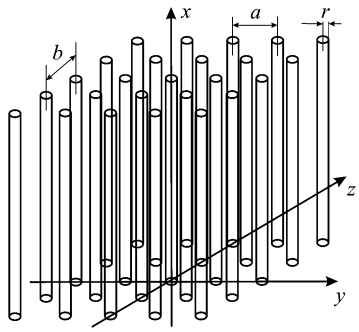

Fig. 1. The geometry of the wire medium: a rectangular lattice of parallel ideally conducting thin wires.

The plasma frequency of wire medium depends on the lattice periods a and b, and on the radius of wires r [5]

$$k_0^2 = \frac{2\pi/(ab)}{\log\frac{\sqrt{ab}}{2\pi r} + F(a/b)} \tag{2}$$

where

$$F(\xi) = -\frac{1}{2}\log\xi + \sum_{n=1}^{+\infty}\left(\frac{\coth(\pi n\xi) - 1}{n}\right) + \frac{\pi}{6}\xi. \tag{3}$$

For the commonly used case of the square grid $(a = b)$, $F(1) = 0.5275$.

The finite-difference time-domain (FDTD) method has been widely used for modelling of transient wave propagation in frequency dispersive and non-dispersive media [6]. The existing frequency dispersive FDTD methods can be categorized into three types: the recursive convolution (RC) method [7], the auxiliary differential equation (ADE) method [8] and the Z-transform method [9]. The RC scheme relates the electric flux density to the electric field intensity through a convolution integral, which can be discretized as a running sum. The dispersive FDTD method applying the RC scheme was used for modelling different types of dispersive materials in [10]–[17]. The ADE method introduces additional differential equation which relates the electric field to the electric current. Through the inverse Fourier transformation and discretization schemes the frequency dependent material properties are taken into account in FDTD modelling. The literatures using the ADE method include [18]–[23]. Another dispersive FDTD method is based on the Z

Manuscript received April 1, 2006; revised August 9, 2006.

The authors are with the Antenna Engineering Group, Queen Mary College, University of London, London E1 4NS, U.K. (e-mail: y.hao@elec.qmul.ac.uk).

Digital Object Identifier 10.1109/TAP.2007.897320

transforms [24]–[26]: the time-domain convolution integral is reduced to a multiplication using the Z-transform, and a recursive relation between electric flux density and electric field is derived.

The simulation of wire medium can be performed either by modelling the physical structures, i.e., parallel wires or through the effective medium approach if the dimension of inclusion is very small compared with the wavelength of operation. However, in order to accurately model thin wires in FDTD, special treatment in the Yee's algorithm (e.g., conformal FDTD [27]) is often needed and leads to requirement for excessive computer resources. Numerical simulations of the structure consisting of an array of 21 by 21 aluminum wires excited by a source in the form of a letter "P" were performed using the CST Microwave Studio [28]. However, the simulation is inadequate when complex sources are considered. The effective medium approach is seen as an efficient alternative when exploring abundant applications of wire medium in antenna and microwave engineering.

In this paper, the effective medium approach is used and the wire medium is modelled as a dielectric material with permittivity of the form (1). Due to the similarity of the frequency and spatial dispersion effects in (1) with Drude material model, the ADE method can be directly applied for the spatially dispersive FDTD modelling.

II. Dispersive FDTD Formulations

Using the (1) the wire media can be modelled in FDTD as a frequency and spatially dispersive dielectric. In order to take into account the dispersive properties of materials in FDTD modelling, the electric flux density is introduced into the standard FDTD updating equations. Since the x-component of electric flux density $D_x(\omega, q_x)$ is related to the x-component of the electric field intensity $E_x(\omega, q_x)$ in the spectral (frequency-wave vector) domain as

$$D_x(\omega) = \varepsilon(\omega, q_x) E_x(\omega) \tag{4}$$

one can write that

$$\left(k^2 - q_x^2\right) D_x + \left(q_x^2 - k^2 + k_0^2\right) \varepsilon_0 E_x = 0. \tag{5}$$

This equation allows to obtain the constitutive relation in the time-space domain in the following form:

$$\left(\frac{\partial^2}{\partial x^2} - \frac{1}{c^2}\frac{\partial^2}{\partial t^2}\right) D_x + \left(\frac{1}{c^2}\frac{\partial^2}{\partial t^2} - \frac{\partial^2}{\partial x^2} + k_0^2\right) \varepsilon_0 E_x = 0 \tag{6}$$

using inverse Fourier transformation and the following rules:

$$k^2 \to -\frac{1}{c^2}\frac{\partial^2}{\partial t^2}, \quad q_x^2 \to -\frac{\partial^2}{\partial x^2}.$$

The (6) relates only x-components of the electric flux density and field intensity. The permittivity in both y- and z-directions is the same as in free space since the wires are assumed to be thin.

The FDTD simulation domain is represented by an equally spaced three-dimensional (3-D) grid with periods Δ_x, Δ_y and Δ_z along x-, y-, and z-directions, respectively. The time step is Δ_t. For discretization of (6), we use the central finite difference operators in time (δ_t^2) and space (δ_x^2) as well as the central average operator with respect to time (μ_t^2)

$$\frac{\partial^2}{\partial t^2} \to \frac{\delta_t^2}{\Delta_t^2}, \quad \frac{\partial^2}{\partial x^2} \to \frac{\delta_x^2}{\Delta_x^2}, \quad k_0^2 \to k_0^2 \mu_t^2$$

where the operators δ_t^2, δ_x^2 and μ_t^2 are defined as in [29]

$$\begin{aligned}
\delta_t^2 F|_{m_x,m_y,m_z}^n &\equiv F|_{m_x,m_y,m_z}^{n+1} - 2F|_{m_x,m_y,m_z}^n \\
&\quad + F|_{m_x,m_y,m_z}^{n-1} \\
\delta_x^2 F|_{m_x,m_y,m_z}^n &\equiv F|_{m_x+1,m_y,m_z}^n - 2F|_{m_x,m_y,m_z}^n \\
&\quad + F|_{m_x-1,m_y,m_z}^n \\
\mu_t^2 F|_{m_x,m_y,m_z}^n &\equiv \left(F|_{m_x,m_y,m_z}^{n+1} + 2F|_{m_x,m_y,m_z}^n \right. \\
&\quad \left. + F|_{m_x,m_y,m_z}^{n-1}\right)/4.
\end{aligned} \tag{7}$$

Here, F represents the field components; m_x, m_y, m_z are indices corresponding to a certain discretization point in the FDTD domain, and n is the number of the time steps. The discretized (6) reads

$$\left(\frac{\delta_x^2}{\Delta_x^2} - \frac{1}{c^2}\frac{\delta_t^2}{\Delta_t^2}\right) D_x + \left(\frac{1}{c^2}\frac{\delta_t^2}{\Delta_t^2} - \frac{\delta_x^2}{\Delta_x^2} + k_0^2\mu_t^2\right) \varepsilon_0 E_x = 0. \tag{8}$$

Note that in (8), the discretization of the term k_0^2 of (6) is performed using the central average operator μ_t^2 in order to guarantee the improved stability. The stability of different discretization schemes is analyzed in details in the next section. The (8) can be written as

$$\begin{aligned}
&\left(\frac{D_x|_{m_x+1,m_y,m_z}^n - 2D_x|_{m_x,m_y,m_z}^n + D_x|_{m_x-1,m_y,m_z}^n}{\Delta_x^2} \right. \\
&\quad \left. \frac{1}{c^2}\frac{D_x|_{m_x,m_y,m_z}^{n+1} - 2D_x|_{m_x,m_y,m_z}^n + D_x|_{m_x,m_y,m_z}^{n-1}}{\Delta_t^2}\right) \\
&\quad + \varepsilon_0 \left(\frac{1}{c^2}\frac{E_x|_{m_x,m_y,m_z}^{n+1} - 2E_x|_{m_x,m_y,m_z}^n + E_x|_{m_x,m_y,m_z}^{n-1}}{\Delta_t^2} \right. \\
&\quad - \frac{E_x|_{m_x+1,m_y,m_z}^n - 2E_x|_{m_x,m_y,m_z}^n + E_x|_{m_x-1,m_y,m_z}^n}{\Delta_x^2} \\
&\quad \left. + k_0^2 \frac{E_x|_{m_x,m_y,m_z}^{n+1} + 2E_x|_{m_x,m_y,m_z}^n + E_x|_{m_x,m_y,m_z}^{n-1}}{4}\right) \\
&\quad = 0.
\end{aligned} \tag{9}$$

Therefore, the updating equation for E_x in terms of E_x and D_x at previous time steps is as follows:

$$\begin{aligned}
&E_x|_{m_x,m_y,m_z}^{n+1} \\
&\quad = \frac{1}{a_{1x}}\left[b_{1x} D_x|_{m_x,m_y,m_z}^{n+1} + b_{2x} D_x|_{m_x+1,m_y,m_z}^n \right. \\
&\quad + b_{3x} D_x|_{m_x,m_y,m_z}^n + b_{4x} D_x|_{m_x-1,m_y,m_z}^n \\
&\quad + b_{5x} D_x|_{m_x,m_y,m_z}^{n-1} - \left(a_{2x} E_x|_{m_x+1,m_y,m_z}^n \right. \\
&\quad + a_{3x} E_x|_{m_x,m_y,m_z}^n + a_{4x} E_x|_{m_x-1,m_y,m_z}^n \\
&\quad \left. \left. + a_{5x} E_x|_{m_x,m_y,m_z}^{n-1}\right)\right]
\end{aligned} \tag{10}$$

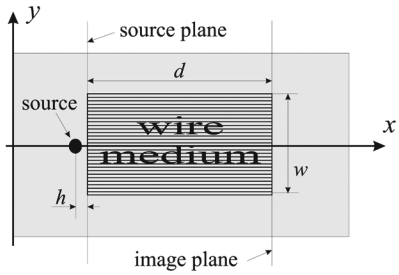

Fig. 2. The layout of the computation domain for two-dimensional FDTD simulations.

with the coefficients given by

$$a_{1x} = -\frac{\varepsilon_0}{c^2\Delta_t^2} - \frac{\varepsilon_0 k_0^2}{4}, \quad b_{1x} = -\frac{1}{c^2\Delta_t^2}$$
$$a_{2x} = \frac{\varepsilon_0}{\Delta_x^2}, \quad b_{2x} = \frac{1}{\Delta_x^2}$$
$$a_{3x} = \frac{2\varepsilon_0}{c^2\Delta_t^2} - \frac{2\varepsilon_0}{\Delta_x^2} - \frac{\varepsilon_0 k_0^2}{2}, \quad b_{3x} = \frac{2}{c^2\Delta_t^2} - \frac{2}{\Delta_x^2}$$
$$a_{4x} = \frac{\varepsilon_0}{\Delta_x^2}, \quad b_{4x} = \frac{1}{\Delta_x^2}$$
$$a_{5x} = -\frac{\varepsilon_0}{c^2\Delta_t^2} - \frac{\varepsilon_0 k_0^2}{4}, \quad b_{5x} = -\frac{1}{c^2\Delta_t^2}.$$

In the spatially dispersive FDTD modelling of wire medium, the calculations of $\mathbf{D}$ from the magnetic field intensity $\mathbf{H}$, and $\mathbf{H}$ from $\mathbf{E}$ are performed using Yee's standard FDTD equations [6], while E_x is calculated from D_x using (10) and $E_y = \varepsilon_0^{-1} D_y$, $E_z = \varepsilon_0^{-1} D_z$. Note that in (10), the central difference approximations in time (for frequency dispersion) for both D_x and E_x are used at position (m_x, m_y, m_z), and the central difference approximations in space (for spatial dispersion) are used at the time step n in order to update E_x at time step $n+1$. Therefore the storage of D_x and E_x at two previous time steps are required.

At the free space-wire medium interfaces along x-direction, the updating (10) includes D_x and E_x at previous time step in both free space and wire medium. Outside the region of wire medium, the updating (10) reduces to the equation relating D_x and E_x in free space.

The spatially dispersive FDTD method has been implemented in a two-dimensional case and used for modelling of sub-wavelength imaging provided by a finite sized slab of wire medium [30]. The simulated geometry is illustrated in Fig. 2. Different types of sources are chosen in simulations including a magnetic point source and three equally spaced magnetic point sources in order to demonstrate the sub-wavelength imaging capability of the device. The simulation results are provided in Section V, while the stability and numerical dispersion relation for general 3-D case are analyzed in the following section.

III. Stability and Numerical Dispersion Analysis

A. Stability

Previous stability analysis of dispersive FDTD schemes is performed using the von Neumann method and numerical root searching [31]. In this paper, the stability of the proposed spatially dispersive FDTD method is analyzed using the method combining the von Neumann method with the Routh-Hurwitz criterion as introduced in [32]. The von Neumann method establishes that, for a finite-difference scheme to be stable, all the roots Z_i of the stability polynomial $S(Z)$ must be inside of the unit circle in the Z-plane (i.e., $|Z_i| \leq 1 \,\forall\, i$), where the complex variable Z corresponds to the growth factor of the error and is often called the amplification factor [32].

The wire medium is a uniaxial material where the divergence of electric field inside wire medium is non-zero ($\nabla \cdot \mathbf{E} \neq 0$). Therefore, to analyze numerical stability of the proposed spatially dispersive FDTD method, we must start directly with the Maxwell's equations instead of the wave equation as was done in [32] and others for the homogeneous materials.

Consider the relation between $\mathbf{D}$ and $\mathbf{E}$ directly expressed from Faraday's and Ampere's Laws

$$\mu_0 \frac{\partial^2 \mathbf{D}}{\partial t^2} + \nabla \times (\nabla \times \mathbf{E}) = 0 \tag{11}$$

where μ_0 is the permeability of free space. Expansion of the matrix form of (11) is

$$\begin{bmatrix} \mu\frac{\partial^2}{\partial t^2} & 0 & 0 \\ 0 & \mu\frac{\partial^2}{\partial t^2} & 0 \\ 0 & 0 & \mu\frac{\partial^2}{\partial t^2} \end{bmatrix} \mathbf{D} + \begin{bmatrix} \frac{\partial^2}{\partial x^2} - \Delta & \frac{\partial}{\partial x}\frac{\partial}{\partial y} & \frac{\partial}{\partial x}\frac{\partial}{\partial z} \\ \frac{\partial}{\partial x}\frac{\partial}{\partial y} & \frac{\partial^2}{\partial y^2} - \Delta & \frac{\partial}{\partial y}\frac{\partial}{\partial z} \\ \frac{\partial}{\partial x}\frac{\partial}{\partial z} & \frac{\partial}{\partial y}\frac{\partial}{\partial z} & \frac{\partial^2}{\partial z^2} - \Delta \end{bmatrix} \mathbf{E} = 0 \tag{12}$$

where

$$\Delta = \frac{\partial^2}{\partial x^2} + \frac{\partial^2}{\partial y^2} + \frac{\partial^2}{\partial z^2}.$$

Using the central difference operators, (12) can be discretized as

$$\mu_0 \frac{\delta_t^2}{\Delta_t^2}\mathbf{D} + \begin{pmatrix} \frac{\delta_x^2}{\Delta_x^2} - \Theta & \frac{\delta_x}{\Delta_x}\frac{\delta_y}{\Delta_y} & \frac{\delta_x}{\Delta_x}\frac{\delta_z}{\Delta_z} \\ \frac{\delta_x}{\Delta_x}\frac{\delta_y}{\Delta_y} & \frac{\delta_y^2}{\Delta_y^2} - \Theta & \frac{\delta_y}{\Delta_y}\frac{\delta_z}{\Delta_z} \\ \frac{\delta_x}{\Delta_x}\frac{\delta_z}{\Delta_z} & \frac{\delta_y}{\Delta_y}\frac{\delta_z}{\Delta_z} & \frac{\delta_z^2}{\Delta_z^2} - \Theta \end{pmatrix} \mathbf{E} = 0 \tag{13}$$

where

$$\Theta = \frac{\delta_x^2}{\Delta_x^2} + \frac{\delta_y^2}{\Delta_y^2} + \frac{\delta_z^2}{\Delta_z^2}$$

and δ_y and δ_z are defined in the same way as in [29]. In addition to the wave equation, the constitutive relation of wire medium (8) must also be considered and can be written in the matrix form

$$\begin{bmatrix} \frac{\delta_x^2}{\Delta_x^2} - \frac{1}{c^2}\frac{\delta_t^2}{\Delta_t^2} & 0 & 0 \\ 0 & -1 & 0 \\ 0 & 0 & -1 \end{bmatrix} \mathbf{D} + \begin{bmatrix} \frac{1}{c^2}\frac{\delta_t^2}{\Delta_t^2} - \frac{\delta_x^2}{\Delta_x^2} + k_0^2 & 0 & 0 \\ 0 & 1 & 0 \\ 0 & 0 & 1 \end{bmatrix} \varepsilon_0 \mathbf{E} = 0. \tag{14}$$

For stability analysis in accordance to [32], we substitute the following solution into the discrete equations (13) and (14)

$$F|^n_{m_x,m_y,m_z} = \tilde{F} Z^n e^{j(m_x\Delta_x\tilde{q}_x + m_y\Delta_y\tilde{q}_y + m_z\Delta_z\tilde{q}_z)} \tag{15}$$

where $\tilde{F}$ is a complex amplitude, Z is the complex variable which gives the growth of the error in a time interation and $\tilde{\mathbf{q}} = (\tilde{q}_x, \tilde{q}_y, \tilde{q}_z)^T$ is the numerical wave vector of the discrete mode. After simple calculations we obtain

$$\begin{aligned} &4Z\begin{bmatrix} \Phi - \frac{\sin^2\theta_x}{\Delta_x^2} & \frac{\sin^2\theta_x}{\Delta_x}\frac{\sin^2\theta_y}{\Delta_y} & \frac{\sin^2\theta_x}{\Delta_x}\frac{\sin^2\theta_z}{\Delta_z} \\ \frac{\sin^2\theta_x}{\Delta_x}\frac{\sin^2\theta_y}{\Delta_y} & \Phi - \frac{\sin^2\theta_y}{\Delta_y^2} & \frac{\sin^2\theta_y}{\Delta_y}\frac{\sin^2\theta_z}{\Delta_z} \\ \frac{\sin^2\theta_x}{\Delta_x}\frac{\sin^2\theta_z}{\Delta_z} & \frac{\sin^2\theta_y}{\Delta_y}\frac{\sin^2\theta_z}{\Delta_z} & \Phi - \frac{\sin^2\theta_z}{\Delta_z^2} \end{bmatrix}\tilde{E} \\ &+ \frac{\mu}{\Delta_t^2}(Z-1)^2\tilde{D} = 0 \end{aligned} \tag{16}$$

where

$$\Phi = \sum_{\alpha=x,y,z} \frac{\sin^2\theta_\alpha}{\Delta_\alpha^2}, \quad \theta_\alpha = \tilde{q}_\alpha\Delta_\alpha/2, \alpha = x,y,z,$$

and

$$\begin{aligned} &\left[-\frac{1}{c^2\Delta_t^2}Z^2 + 2\left(\frac{1}{c^2\Delta_t^2} - \frac{2\sin^2\theta_x}{\Delta_x^2}\right)Z - \frac{1}{c^2\Delta_t^2}\right]\tilde{D}_x \\ &+ \left[\left(\frac{1}{c^2\Delta_t^2} + \frac{k_0^2}{4}\right)Z^2 + \left(-\frac{2}{c^2\Delta_t^2} + \frac{4\sin^2\theta_x}{\Delta_x^2} + \frac{k_0^2}{2}\right)Z \right. \\ &\left. + \left(\frac{1}{c^2\Delta_t^2} + \frac{k_0^2}{4}\right)\right]\varepsilon_0\tilde{E}_x = 0 \\ &\tilde{D}_y - \varepsilon_0\tilde{E}_y = 0, \quad \tilde{D}_z - \varepsilon_0\tilde{E}_z = 0 \end{aligned} \tag{17}$$

respectively. The determinant of the system of equations (16) and (17) provides us with the stability polynomial

$$\begin{aligned} S_w(Z) = &\left(\frac{1}{c^2\Delta_t^2} + \frac{k_0^2}{4}\right)Z^4 \\ &+ 4\left(-\frac{1}{c^2\Delta_t^2} + \frac{\sin^2\theta_x}{\Delta_x^2} + \Phi\right)Z^3 \\ &+ \left[\frac{6}{c^2\Delta_t^2} - \frac{k_0^2}{2} - \frac{8\sin^2\theta_x}{\Delta_x^2} \right. \\ &- 8\left(1 - \frac{2c^2\Delta_t^2\sin^2\theta_x}{\Delta_x^2}\right)\Phi \\ &\left. + \frac{4k_0^2c^2\Delta_t^2\sin^2\theta_x}{\Delta_x^2}\right]Z^2 \\ &+ 4\left(-\frac{1}{c^2\Delta_t^2} + \frac{\sin^2\theta_x}{\Delta_x^2} + \Phi\right)Z \\ &+ \left(\frac{1}{c^2\Delta_t^2} + \frac{k_0^2}{4}\right). \end{aligned} \tag{18}$$

For simplicity, the terms that will lead to the stability condition in free space (i.e., the conventional stability condition) are omitted from this stability polynomial.

In order to avoid numerical root searching [31] for obtaining the stability conditions, the above stability polynomial can be transformed into the r-plane using the bilinear transformation

$$Z = \frac{r+1}{r-1}. \tag{19}$$

The stability polynomial in the r-plane becomes as follows:

$$\begin{aligned} S_w(r) = &\left(\frac{4c^2\Delta_t^2\sin^2\theta_x}{\Delta_x^2}\Phi + \frac{k_0^2c^2\Delta_t^2\sin^2\theta_x}{\Delta_x^2}\right)r^4 \\ &+ \left[k_0^2 + \frac{4\sin^2\theta_x}{\Delta_x^2} + 4\left(1 - \frac{2c^2\Delta_t^2\sin^2\theta_x}{\Delta_x^2}\right)\Phi \right. \\ &\left. - \frac{2k_0^2c^2\Delta_t^2\sin^2\theta_x}{\Delta_x^2}\right]r^2 \\ &+ \left[\frac{4}{c^2\Delta_t^2} - \frac{4\sin^2\theta_x}{\Delta_x^2} - 4\left(1 - \frac{c^2\Delta_t^2\sin^2\theta_x}{\Delta_x^2}\right)\Phi \right. \\ &\left. + \frac{k_0^2c^2\Delta_t^2\sin^2\theta_x}{\Delta_x^2}\right]. \end{aligned} \tag{20}$$

Building up the Routh table for the above polynomial as in [32], we obtain the following stability conditions:

$$\begin{aligned} &\frac{4\sin^2\theta_x}{\Delta_x^2}\left(1 - c^2\Delta_t^2\Phi\right) + 4\left(1 - \frac{c^2\Delta_t^2\sin^2\theta_x}{\Delta_x^2}\right)\Phi \\ &+ k_0^2\left(1 - \frac{2c^2\Delta_t^2\sin^2\theta_x}{\Delta_x^2}\right) \geq 0 \end{aligned} \tag{21}$$

$$\begin{aligned} &4\left(\frac{1}{c^2\Delta_t^2} - \frac{\sin^2\theta_x}{\Delta_x^2}\right)\left(1 - c^2\Delta_t^2\Phi\right) \\ &+ \frac{k_0^2c^2\Delta_t^2\sin^2\theta_x}{\Delta_x^2} \geq 0. \end{aligned} \tag{22}$$

In order to fulfil these conditions, it is enough to fulfil the conventional Courant stability condition [6]

$$\Delta_t \leq \frac{1}{c\Phi^{1/2}} \leq \frac{1}{c}\left(\sum_{\alpha=x,y,z}\frac{1}{\Delta_\alpha^2}\right)^{-1/2}. \tag{23}$$

Therefore, the conventional Courant stability condition [6] is preserved for modelling of wire medium and no additional conditions are required.

Note that in the above analysis, the central average operator μ_t^2 was used for discretization of the (6). If we choose the central average operator μ_{2t} defined as

$$\mu_{2t}F|^n_{m_x,m_y,m_z} = \left(F|^{n+1}_{m_x,m_y,m_z} + F|^{n-1}_{m_x,m_y,m_z}\right)/2 \tag{24}$$

then the stability condition (21) remains the same, but (22) becomes

$$\begin{aligned} &4\left(\frac{1}{c^2\Delta_t^2} - \frac{\sin^2\theta_x}{\Delta_x^2}\right)\left(1 - c^2\Delta_t^2\Phi\right) \\ &+ k_0^2\left(1 + \frac{c^2\Delta_t^2\sin^2\theta_x}{\Delta_x^2}\right) \geq 0 \end{aligned} \tag{25}$$

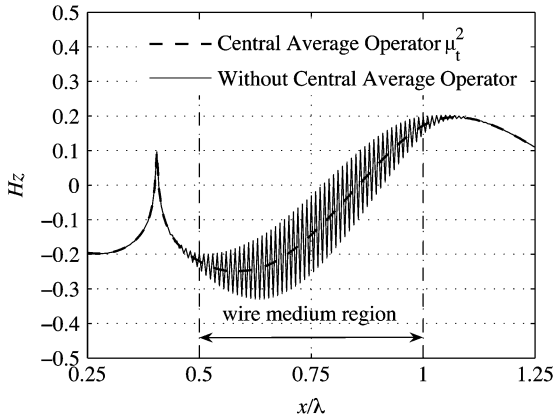

Fig. 3. Comparison of the internal magnetic field distributions (unit: A/m) in the plane $y = 0$ for a wire medium slab excited by a point magnetic source ($d = 0.5\lambda$, $w = \lambda$, $h = 0.1\lambda$ and $k_0/k = 4$) calculated using different discretization schemes: dashed line—the central average operator μ_t^2, solid line—without using central average operator. The field is plotted at the time step $n = 570\Delta_t$, where Δ_t is chosen as the Courant limit i.e., $\Delta_t = \Delta_x/\sqrt{2}c$, $\Delta_x = \lambda/200$.

which indicates that even less restrictive stability condition than that for the conventional FDTD method can be reached. However, if no central average operator is used when discretizing the (6), then (21) also remains the same, but (22) will change to

$$\left(\frac{1}{c^2\Delta_t^2} - \frac{\sin^2\theta_x}{\Delta_x^2}\right)\left[4\left(1 - c^2\Delta_t^2\Phi\right) - k_0^2c^2\Delta_t^2\right] \geq 0. \quad (26)$$

Therefore, if the plasma frequency used in simulations is too high and the time step is not properly chosen, then the discretized formulations can become unstable. Fig. 3 shows the comparison of magnetic field distribution using different discretization schemes: using the central average operator μ_t^2 and without using central average operator. It is clearly shown that after 500 time steps, the instability errors start appearing from inside the wire medium slab using the latter scheme.

B. Numerical Dispersion

The numerical dispersion relation for the wire medium can be found by evaluating the stability polynomial $S_w(Z)$ given by (18) on the unit circle of the Z-plane (i.e., by letting $Z = e^{j\omega\Delta_t}$), and equating the results to zero. After some calculations, the numerical dispersion relation for wire medium is obtained

$$\left(\frac{4}{c^2\Delta_t^2} + k_0^2\right)\sin^4\frac{\omega\Delta_t}{2} - \left(\frac{4\sin^2\theta_x}{\Delta_x^2} + k_0^2\right)\sin^2\frac{\omega\Delta_t}{2} + \frac{k_0^2c^2\Delta_t^2\sin^2\theta_x}{\Delta_x^2} = 4\left(\sin^2\frac{\omega\Delta_t}{2} - c^2\Delta_t^2\frac{\sin^2\theta_x}{\Delta_x^2}\right)\Phi. \quad (27)$$

If $\Delta_\beta \to 0$, where $\beta = x, y, z, t$, then (27) reduces to the continuous dispersion relation for wire medium [4]

$$\left(q_x^2 - k^2\right)\left(q_x^2 + q_y^2 + q_z^2 - k^2 + k_0^2\right) = 0. \quad (28)$$

The first and second terms of (28) correspond to the transmission line modes (TEM waves with respect to the orientation of wires) and the extraordinary modes (TM waves), see [4] for details. The ordinary modes (TE waves) do not appear in (28) since their contribution was omitted in (18) for simplicity of calculation.

IV. Perfectly Matched Layer Formulation

In 1994, Berenger introduced a nonphysical absorber for terminating the outer boundaries of the FDTD computation domain that has a wave impedance independent of the angle of incidence and frequency. This absorber is called the perfectly matched layer (PML) [33]. The development of PML involves a splitting-field approach and the reflection from a PML boundary is dependent only on the PML's depth and conductivity. In [34], Berenger's original PML is extended to absorb electromagnetic waves propagating in anisotropic dielectric and magnetic media by introducing the material-independent quantities (electric flux density $\mathbf{D}$ and magnetic flux density $\mathbf{B}$).

PMLs are usually placed at a distance of $\lambda/2$ from any objects in the simulation domain. In order to reduce the time and computer memory requirements for simulations as well as to improve the convergence performance, it is required to place the PML in the close vicinity of the wire medium. For that purpose, we can follow a similar approach as in [34] by modifying Berenger's original PML formulations. In the modified PML for wire medium, $\mathbf{D}$ is introduced into the updating equations and the quantities $\mathbf{D}$ and $\mathbf{H}$ are splitted. For example, the updating equation for D_{zx} becomes

$$D_{zx}|_{m_x,m_y,m_z}^{n+1} = e^{-\sigma_x^D\Delta t}D_{zx}|_{m_x,m_y,m_z}^{n} + \frac{\left(1 - e^{-\sigma_x^D\Delta t}\right)}{-\sigma_x^D\Delta x} \times \left[H_y|_{m_x+1/2,m_y,m_z}^{n+1/2} - H_y|_{m_x-1/2,m_y,m_z}^{n+1/2}\right] \quad (29)$$

and the updating equations for $\mathbf{H}$ remain the same as in Berenger's original PML [33]. The matching conditions are

$$\sigma_\alpha^D = \sigma_\alpha^H, \quad \text{where } \alpha = x, y, z \quad (30)$$

where σ_α^D and σ_α^H denote electric conductivity and magnetic loss inside the PML, respectively. It should be noted that the difference between the above expressions and Berenger's original PML formulations is that ε_0 is not involved in the expression of the theoretical reflection factor $R(\theta)$ for σ_α^D [34]. Furthermore, the updating relation between $\mathbf{D}$ and $\mathbf{E}$ in (10) must be extended into the PML in order to match wire medium with the modified PML.

In order to evaluate the performance of the modified PML for the wire medium, a 2-D computation domain similar to that in Fig. 2 is chosen except that along y-direction where the wire medium slab is directly terminated by a ten-cell modified PML (MPML) with a normal theoretical reflection $R(0) = 10^{-5}$ (see sketch in Fig. 4). From the other sides the Berenger's original PML is used to truncate the free space. The source is located close to the edge of the wire medium slab terminated by MPML and enough far away to the other side of the slab in order to ensure that the wave reflected back from that side does not reach the reference plane during calculations. The observation plane is 2 cells away from the MPML. The reference plane is located at the same distance from the source as the observation plane, but from the other side (see sketch in Fig. 4). The magnetic fields at

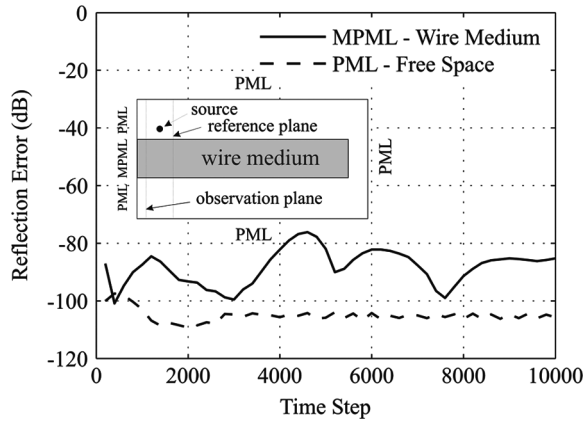

Fig. 4. Reflection error (in dB) from the MPML-wire medium and PML-free space interfaces calculated at the observation plane (2 cells away from the PMLs) for a wire medium slab excited by a point magnetic source ($d = 0.5\lambda$, $h = 0.1\lambda$ and $k_0/k = 4$) plotted as functions of the time step. The wire medium along y-direction is long enough to ensure the wave reflected back from the far boundary does not reach the reference plane during calculations.

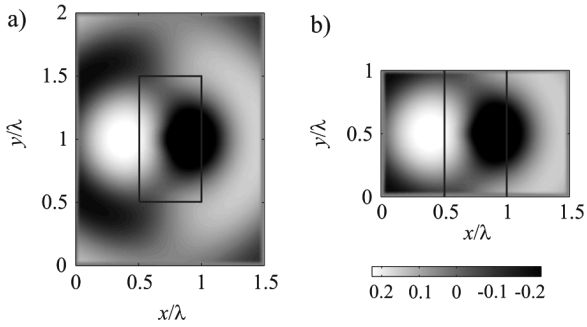

Fig. 5. (a) Distribution of magnetic field for a finite wire medium slab excited by a point magnetic source ($d = 0.5\lambda$, $w = \lambda$, $h = 0.1\lambda$ and $k_0/k = 4$). (b) The same slab, but terminated by a ten-cell MPML at each side along y-direction (unit: A/m).

the observation and reference planes are recorded as $H_{\rm PML}$ and $H_{\rm ref}$, respectively. The reflection error is defined as

$$\text{Reflection Error (dB)} = 20\times\log_{10}\left(\frac{|H_{\rm PML} - H_{\rm ref}|}{|H_{\rm max}|}\right) \quad (31)$$

where $|H_{\rm max}|$ is the maximum value of the magnetic field at the reference plane. The reflection error is then calculated for H_z and shown in Fig. 4. For comparison, the reflection error at the PML-free space interface is also shown. It is found that the reflections from the PML are less than -70 dB thus the wire medium is "perfectly" matched.

Fig. 5 shows the comparison of magnetic field distributions for two cases: using Berenger's original PML at $\lambda/2$ distance from the slab and using the modified PML to truncate the wire medium slab directly. In comparison with Fig. 5(a), the simulation domain size for Fig. 5(b) is reduced by 50% and the convergence is greatly improved since the diffractions from the corners and edges are avoided in simulations. For the first case, the reflection error falls below -30 dB after 1000 periods (400 000 time steps), while for the latter one, the convergence is reached after 100 periods.

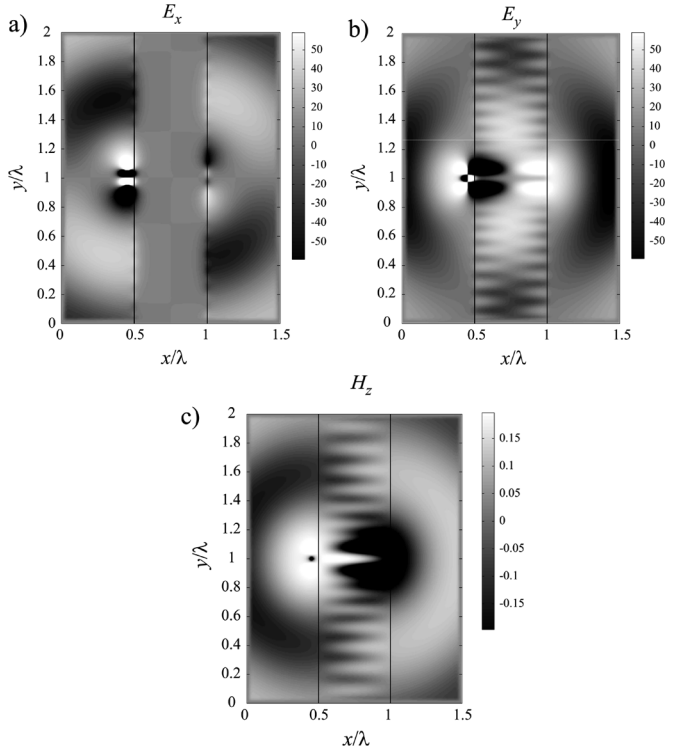

Fig. 6. The distributions of (a) E_x (unit: V/m), (b) E_y (unit: V/m), and (c) H_z (unit: A/m) for a wire medium slab excited by three equally spaced magnetic sources with the phase differences equal to π ($d = 0.5\lambda$, $h = 0.05\lambda$ and $k_0/k = 4$) directly terminated by a ten-cell MPML at each side along y-direction.

V. Modelling of the Sub-Wavelength Imaging

In order to validate the proposed spatially dispersive FDTD formulations, we have chosen flat sub-wavelength lenses formed by wire media [30], [28]. Such lenses provide unique opportunity to transfer images with resolution below classical diffraction limit. In the present paper we have considered a 2-D case: the structure is infinite in z-direction and electric field is in $x - y$ plane (TM polarization with respect to the orientation of wires). The following parameters are used in simulations: the operating frequency is 3.0 GHz (wavelength $\lambda = 0.1$ m in free space) and the plasma frequency of the wire medium is $f_0 = 12.0$ GHz ($k_0/k = 4$); the FDTD cell size is $\Delta_x = \lambda/200$ with the time step $\Delta_t = 8.33 \times 10^{-13}$s according to the stability criteria (23); a ten-cell Berenger's original PML is used to truncate the free space and the modified PML (MPML) is used to match the wire medium slab; the thickness of the wire media slab is chosen as $d = \lambda/2$. Three equally spaced ($\lambda/20$) magnetic point sources with phase differences of 180° between neighboring sources are located at a distance of $\lambda/20$ from the left interface of the wire medium slab.

Fig. 6 shows the distribution of the x- and y- components of electric field as well as z- component of magnetic field in the simulation domain. One can see from Fig. 6(a) that x-component of electrical field penetrates into the wire medium in the form of extraordinary modes [4] which are evanescent and decay with distance. That is why this component vanishes in the center of the slab. The extraordinary modes are coupled with transmission line modes of wire medium which are clearly seen

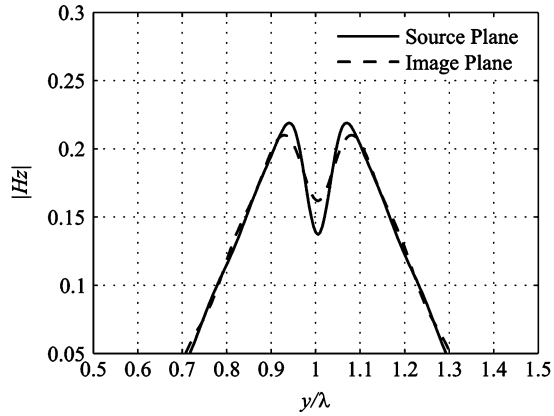

Fig. 7. Comparison of magnetic field distribution at the source and image planes for a wire medium slab ($d = 0.5\lambda, h = 0.05\lambda$ and $k_0/k = 4$) directly terminated by a ten-cell MPML at each side along y-direction. (unit: A/m)

in Fig. 6(b) and (c). In accordance to the canalization principle [30], the transmission line modes deliver image from the front interface to the back one. Fig. 7 shows the magnetic field distribution at the source and image planes (located on the different sides of wire medium slab as in Fig. 2). It is worth noting that the image is in phase or out-of-phase with the source if the thickness of wire medium slab is even or odd integer numbers of $\lambda/2$, respectively [30]. That is why in the case under consideration the image appears in out of phase. It can be seen that in Fig. 7 the distance between two maxima is approximately $\lambda/10$ which verifies the sub-wavelength imaging capability of the wire medium lenses. The performed simulations confirm that the spatial dispersion in wire medium is accurately taken into account in the presented spatially dispersive FDTD model.

VI. Conclusion

The spatially dispersive FDTD formulations have been developed for modelling of wave propagation in wire medium as effective dielectrics. The auxiliary differential equation method is used in order to take into account both the spatial and frequency dispersion effects. The stability analysis shows that the conventional Courant stability limit is preserved if the standard central difference approximations and central average operator are used to discretize differential equations. Through the use of modified PML, the wire medium can be "perfectly" matched to the absorbing boundaries thus the convergence performance in simulations is greatly improved since the diffractions from corners and edges of the finite sized wire medium slab are avoided. The flat sub-wavelength lenses formed by wire medium are chosen for the validation of developed spatially dispersive FDTD formulations. Numerical simulation results verifies the sub-wavelength imaging capability of wire media. The proposed spatially dispersive FDTD method will demonstrate its distinct value when complex sources are used in the simulation for exploitation of practical applications of wire medium in antenna and microwave engineering.

References

[1] J. Brown, "Artificial dielectrics," *Progress in Dielectrics*, vol. 2, pp. 195–225, 1960.

[2] W. Rotman, "Plasma simulations by artificial dielectrics and parallel-plate media," *IRE Trans. Antennas Propag.*, vol. 10, pp. 82–95, 1962.

[3] J. B. Pendry, A. J. Holden, W. J. Steward, and I. Youngs, "Extremely low frequency plasmons in metallic mesostructures," *Phys. Rev. Lett.*, vol. 76, pp. 4773–4776, 1996.

[4] P. A. Belov, R. Marques, S. I. Maslovski, I. S. Nefedov, M. Silveirinha, C. R. Simovski, and S. A. Tretyakov, "Strong spatial dispersion in wire media in the very large wavelength limit," *Phys. Rev. B*, vol. 67, pp. 113103(1)–113103(4), 2003.

[5] P. A. Belov, S. A. Tretyakov, and A. J. Viitanen, "Dispersion and reflection properties of artificial media formed by regular lattices of ideally conducting wires," *J. Electromagn. Waves Applic.*, vol. 16, pp. 1153–1170, 2002.

[6] A. Taflove, *Computational Electrodynamics: The Finite Difference Time Domain Method*. Norwood, MA: Artech House, 1995.

[7] R. Luebbers, F. P. Hunsberger, K. Kunz, R. Standler, and M. Schneider, "A frequency-dependent finite-difference time-domain formulation for dispersive materials," *IEEE Trans. Electromagn. Compat.*, vol. 32, pp. 222–227, Aug. 1990.

[8] O. P. Gandhi, B.-Q. Gao, and J.-Y. Chen, "A frequency-dependent finite-difference time-domain formulation for general dispersive media," *IEEE Trans. Microw. Theory Tech.*, vol. 41, pp. 658–664, Apr. 1993.

[9] D. M. Sullivan, "Frequency-dependent FDTD methods using Z transforms," *IEEE Trans. Antennas Propag.*, vol. 40, pp. 1223–1230, Oct. 1992.

[10] R. J. Luebbers, F. Hunsberger, and K. S. Kunz, "A frequency-dependent finite-difference time-domain formulation for transient propagation in plasma," *IEEE Trans. Antennas Propag.*, vol. 39, no. 1, pp. 29–34, 1991.

[11] R. J. Luebbers and F. Hunsberger, "FDTD for Nth-order dispersive media," *IEEE Trans. Antennas Propag.*, vol. 40, no. 11, pp. 1297–1301, 1992.

[12] F. Hunsberger, R. J. Luebbers, and K. S. Kunz, "Finite-difference time-domain analysis of gyrotropic media. I: Magnetized plasma," *IEEE Trans. Antennas Propag.*, vol. 40, no. 12, pp. 1489–1495, 1992.

[13] C. Melon, P. Leveque, T. Monediere, A. Reineix, and F. Jecko, "Frequency dependent finite-difference-time-domain formulation applied to ferrite material," *Microwave Opt. Technol. Lett.*, vol. 7, no. 12, pp. 577–579, 1994.

[14] A. Akyurtlu and D. H. Werner, "BI-FDTD: A novel finite-difference time-domain formulation for modeling wave propagation in bi-isotropic media," *IEEE Trans. Antennas Propag.*, vol. 52, no. 2, pp. 416–425, 2004.

[15] A. Grande, I. Barba, A. Cabeceira, J. Represa, P. So, and W. Hoefer, "FDTD modeling of transient microwave signals in dispersive and lossy bi-isotropic media," *IEEE Trans. Microw. Theory Tech.*, vol. 52, no. 3, pp. 773–784, 2004.

[16] A. Akyurtlu and D. H. Werner, "A novel dispersive FDTD formulation for modelling transient propagation in chiral metamaterials," *IEEE Trans. Antennas Propag.*, vol. 52, no. 9, pp. 2267–2276, 2004.

[17] J.-Y. Lee, J.-H. Lee, H.-S. Kim, N.-W. Kang, and H.-K. Jung, "Effective medium approach of left-handed material using a dispersive FDTD method," *IEEE Trans. Magn.*, vol. 41, no. 5, pp. 1484–1487, 2005.

[18] T. Kashiwa, N. Yoshida, and I. Fukai, "A treatment by the finite-difference time-domain method of the dispersive characteristics associated with orientation polarization," *Trans. IEICE*, vol. E73, no. 8, pp. 1326–1328, 1990.

[19] T. Kashiwa and I. Fukai, "A treatment by the FD-TD method of the dispersive characteristics associated with electronic polarization," *Microw. Opt. Technol. Lett.*, vol. 3, no. 6, pp. 203–205, 1990.

[20] P. M. Goorjian and A. Taflove, "Direct time integration of Maxwell's equations in nonlinear dispersive media for propagation and scattering of femtosecond electromagnetic solitons," *Opt. Lett.*, vol. 17, no. 3, pp. 180–182, 1992.

[21] O. P. Gandhi, B. Q. Gao, and J. Y. Chen, "A frequency-dependent finite-difference time-domain formulation for induced current calculations in human beings," *Bioelectromagn.*, vol. 13, no. 6, pp. 543–556, 1992.

[22] O. P. Gandhi, B. Q. Gao, and J. Y. Chen, "A frequency-dependent finite-difference time-domain formulation for general dispersive media," *IEEE Trans. Microw. Theory Tech.*, vol. 41, no. 4, pp. 658–665, 1993.

[23] L. Lu, Y. Hao, and C. Parini, "Dispersive FDTD characterisation of no phase-delay radio transmission over layered left-handed meta-materials structure," *Proc. Inst. Elect. Eng. Sci. Meas. Technol.*, vol. 151, no. 6, pp. 403–406, Nov. 2004.

[24] D. M. Sullivan, "Nonlinear FDTD formulations using Z transforms," *IEEE Trans. Microw. Theory Tech.*, vol. 43, no. 3, pp. 676–682, 1995.

[25] V. Demir, A. Z. Elsherbeni, and E. Arvas, "FDTD formulation for dispersive chiral media using the Z transform method," *IEEE Trans. Antennas Propag.*, vol. 53, no. 10, pp. 3374–3384, 2005.
[26] M. W. Feise, J. B. Schneider, and P. J. Bevelacqua, "Finite-difference and pseudospectral time-domain methods applied to backward-wave metamaterials," *IEEE Trans. Antennas Propag.*, vol. 52, no. 11, pp. 2955–2962, 2004.
[27] Y. Hao and C. J. Railton, "Analyzing electromagnetic structures with curved boundaries on cartesian FDTD meshes," *IEEE Trans. Microw. Theory Tech.*, vol. 46, no. 1, pp. 82–88, Jan. 1998.
[28] P. A. Belov, Y. Hao, and S. Sudhakaran, "Subwavelength microwave imaging using an array of parallel conducting wires as a lens," *Phys. Rev. B*, vol. 73, pp. 033108(1)–033108(4), 2006.
[29] F. B. Hildebrand, *Introduction to Numerical Analysis*. New York: McGraw-Hill, 1956.
[30] P. A. Belov, C. R. Simovski, and P. Ikonen, "Canalisation of sub-wavelength images by electromagnetic crystals," *Phys. Rev. B*, vol. 71, pp. 193105(1)–193105(4), 2005.
[31] P. G. Petropoulos, "Stability and phase error analysis of FD-TD in dispersive dielectrics," *IEEE Trans. Antennas Propag.*, vol. 42, pp. 62–69, Jan. 1994.
[32] A. Pereda, L. A. Vielva, A. Vegas, and A. Prieto, "Analyzing the stability of the FDTD technique by combining the von Neumann method with the Routh-Hurwitz criterion," *IEEE Trans. Microw. Theory Tech.*, vol. 49, no. 2, pp. 377–381, Feb. 2001.
[33] J. R. Berenger, "A perfectly matched layer for the absorption of electromagnetic waves," *J. Computat. Phys.*, vol. 114, pp. 185–200, Oct. 1994.
[34] A. P. Zhao, "Generalized-material-independent PML absorbers used for the FDTD simulation of electromagnetic waves in 3-D arbitrary anisotropic dielectric and magnetic media," *IEEE Trans. Microw. Theory Tech.*, vol. 46, no. 10, pt. 1, pp. 1511–1513, Oct. 1998.

Yan Zhao (S'03) received the B.Sc. degree from Beijing University of Posts and Telecommunications (BUPT), China, in 2002 and the M.Sc. degree from The University of Birmingham, U.K., in 2003. He is currently working toward the Ph.D. degree at Queen Mary, University of London.

His main research interests include finite-difference time-domain (FDTD) modelling of dispersive materials, ultrawideband (UWB) radio systems, and human interactions with indoor radio channels.

Pavel A. Belov (S'99–M'03) received the B.S., M.S., and Ph.D. degrees from St. Petersburg Institute of Fine Mechanics and Optics, Russia, in 1998, 2000, and 2003, respectively.

He was a Researcher in the Radio Laboratory of Helsinki University of Technology, Finland, from 2001 to 2003, an Associate Professor in the Photonics and Optoinformatics Department at St. Petersburg State University of Information Technologies, Mechanics and Optics, Russia, from 2003 to 2004, and a Research Engineer in the Telecommunication Division at Samsung Electronics Ltd., Korea, from 2004 to 2005. Since 2005, he has been a Postdoctoral Research Assistant in the Electronic Engineering Department at Queen Mary, University of London, U.K. His research interests include analytical and numerical modeling of metamaterials, photonic and electromagnetic crystals, artificial dielectrics and magnetics, as well as microwave, terahertz and optical subwavelength imaging using the metamaterials.

Yang Hao (M'99–SM'06) received the Ph.D. degree from the Centre for Communications Research (CCR), University of Bristol, Bristol, U.K., in 1998.

From 1998 to 2000, he was a Postdoctoral Research Fellow in the School of Electrical and Electronic Engineering, University of Birmingham, U.K. In May 2000, he joined the Antenna Engineering Group, Queen Mary College, University of London, London, U.K., first as a Lecturer and now a Reader in antennas and electromagnetics. He has coedited a book, contributed two book chapters and published over 60 technical papers. His research interests are computational electromagnetics, on-body radio propagations, active integrated antennas, electromagnetic bandgap structures and microwave metamaterials.

Dr. Hao is a Member of the Institution of Electrical Engineers (IEE), London, U.K. He is also a member of the Technical Advisory Panel of the IEE Antennas and Propagation Professional Network and a member of the Wireless Onboard Spacecraft Working Group, ESTEC, ESA. He was a session organizer and chair for various international conferences and also a keynote speaker at ANTEM 2005, France.